

Electronic Supplementary Information

Magnetic bistability of TbPc₂ submonolayer on a graphene/SiC(0001) conductive electrode.

G. Serrano,^{a*} E. Velez-fort,^{b*} I. Cimatti,^a B. Cortigiani,^a L. Malavolti,^{c,d} D. Betto,^b A. Ouerghi,^e N. B. Brookes,^b M. Mannini,^{a*} and R. Sessoli^a

^a Department of Chemistry and INSTM RU, University of Florence, Via della Lastruccia 3, 50019, Sesto Fiorentino (FI), Italy.

E-mail: giulia.serrano@unifi.it; matteo.mannini@unifi.it

^b European Synchrotron Radiation Facility, 71, avenue des Martyrs CS 40220, 38043 Grenoble Cedex 9, France
E-mail : emilio.velez-fort@esrf.fr.

^c Max-Planck Department for Structural Dynamics Luruper Chaussee 149, 22761 Hamburg, Germany.

^d Max-Planck Institute for Solid State Research, Heisenbergstrasse. 1, 70569 Stuttgart, Germany.

^e Centre de Nanosciences et de Nanotechnologies, CNRS, Université Paris-Sud, Université Paris-Saclay, C2N–Marcoussis, 91460 Marcoussis, France.

1. Experimental Methods

1.1 Synthesis of the graphene substrate

The graphene has been prepared using the method of graphitization of silicon carbide as described in literature (see Methods of Pallecchi et al.¹). We employed a 6H-SiC(0001) substrate with a nitrogen doping level of 10¹⁷ cm⁻³. This method leads to the formation of graphene layers on top of an electrically dead layer at the interface with the SiC(0001) surface, called interface layer.

1.2 Synthesis of the TbPc₂ molecules

The neutral bis(phthalocyaninato)terbium molecules were synthesized by mixing the corresponding lanthanide acetate with 1,2-dicyanobenzene in the presence of a catalytic amount of 1,8-diazabicyclo[5.4.0]undec-7-ene following the procedure reported in the literature.^{2,3} A further purification of the powder has been obtained by means of UHV sublimation process before the molecular deposition.

1.3 Sample preparation and characterization methods

The substrates used for molecular deposition were the graphene/SiC(0001), described in the first section of the ESI, and a clean 6H-SiC(0001) sample. The graphene and the 6H-SiC(0001) substrates were annealed at 770-830 K for about 1 hour before molecular deposition in order to remove surface contaminations. This annealing temperature range avoids any modification of the surface reconstruction.⁴ The SiC(0001) and the graphene substrates were characterized by Low Energy Electron Diffraction (LEED) at the ID32 beamline before molecular deposition (see Figure S1). The SiC(0001) substrate has been also characterized by Atomic Force Microscopy (AFM) at the ESRF (see Figure S1). The same substrate preparation procedure was carried out also at the CETECS laboratory at the Department of Chemistry of the University of Florence using similar working conditions to prepare substrates for in-house analyses. Core-level X-ray Photoelectron Spectroscopy (XPS) was used to characterize the graphene/SiC(0001) substrate (see Figure S2). The XPS data were acquired using monochromatic Al K_{α} radiation ($h\nu = 1486.7$ eV) SPECS mod. XR-MS focus 600 and a SPECS Phoibos 150 electron analyzer in normal emission with the X-ray source mounted at an angle of 54.44° with respect to the analyzer. XPS spectra were measured at normal and grazing (with an angle of 60°) emission with a fixed pass energy of 40 eV. The inelastic background in the spectra was subtracted by means of the Shirley method. The deconvolution of the XPS spectra was carried out using the product of Gaussian and Lorentzian line shapes for each component in the spectra. The spectra were calibrated by placing the SiC component of the C1s spectra at 283.4 eV, as reported in literature.⁵

TbPc₂ molecules were deposited via sublimation in UHV at 680 K in order to obtain a submonolayer coverage of 0.6 ML. During the molecular deposition, the substrate was kept at room temperature. Same deposition parameters have been used at the CETECS laboratory and at the ID32 beamline. Calibration and STM characterization of the molecular deposition has been carried out at the CETECS laboratory. To calibrate the molecular coverage, a Quartz Crystal Microbalance (QCM) has been used flanked by *in situ* STM investigation of molecular films grown on an Au(111) crystal, previously prepared by sputtering and annealing. The STM analysis of the TbPc₂ on graphene has been carried out in house by using an Omicron VT-STM. STM measurements were carried out at 35 K in order to stabilize the molecules on the surface during the STM scan and using chemically etched W tips, annealed in vacuum before the measurements. To compare the deposition conditions obtained at the laboratory in Florence and at the ESRF facility we have calibrated the molecular coverage by STM measurements using a common reference substrate, *i.e.* an Au(111) crystal cleaned in UHV with the same method.

X-ray adsorption magnetic measurements were performed at the ID32 beamline of the ESRF synchrotron facility. The sample was prepared in UHV exploiting the preparation chamber of the beamline, which allows the transfer of the sample to the chamber used for the measurements without breaking the vacuum. To obtain similar coverage and similar experimental conditions for the two investigated substrates, they were mounted on the same sample-holder and TbPc₂ was simultaneously sublimated on both of them.

2. Substrate characterization

In order to confirm the quality of the surface of our substrates before the deposition of the molecules, we used LEED and AFM. Figure S1 shows the LEED patterns of the pristine SiC(0001) (a) and the graphene grown on SiC(0001) (b). Black and red arrows indicate the SiC and graphene diffraction spots, respectively. Blue arrows indicate additional spots due to the interface layer between the graphene and the SiC substrate.⁶ AFM images are shown in Figure S1 for (c) the clean 6H-SiC(0001) substrate and (d) graphene on 6H-SiC(0001), evidencing the presence of steps of 0.6 nm height and 400 nm width for the SiC clean surface and showing that graphene covers the whole wafer, forming terraces of 4-6 nm height and 1-2 μm width.

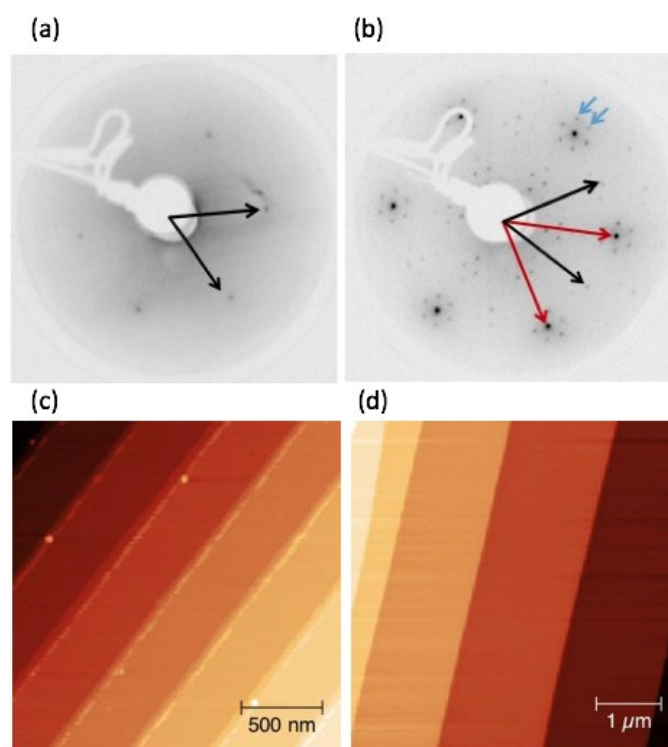


Figure S1. LEED images of (a) SiC(0001) at 97 eV and (b) Graphene/SiC(0001) at 95 eV. The AFM images of the respective substrates are shown in panel (c) and (d).

XPS has been used to check the chemical properties of the clean graphene sample. Figure S2 panel a, shows the XPS survey scan measured on the clean graphene/SiC substrate: only Si and C related peaks are present, confirming the cleanliness of the surface. The C 1s peaks at normal (panel b) and grazing incidence angle of 60° between the sample and the X-ray source (panel c) show three components at 283.4, 284.3 and $285.3 \pm 0.2\text{eV}$. These components correspond to the SiC bulk (red), the graphene layer

(blue) and the interface layer (green), respectively, in remarkable agreement with the literature.⁵ As expected the component at 284.3 eV, representing graphene, increases at grazing incidence.

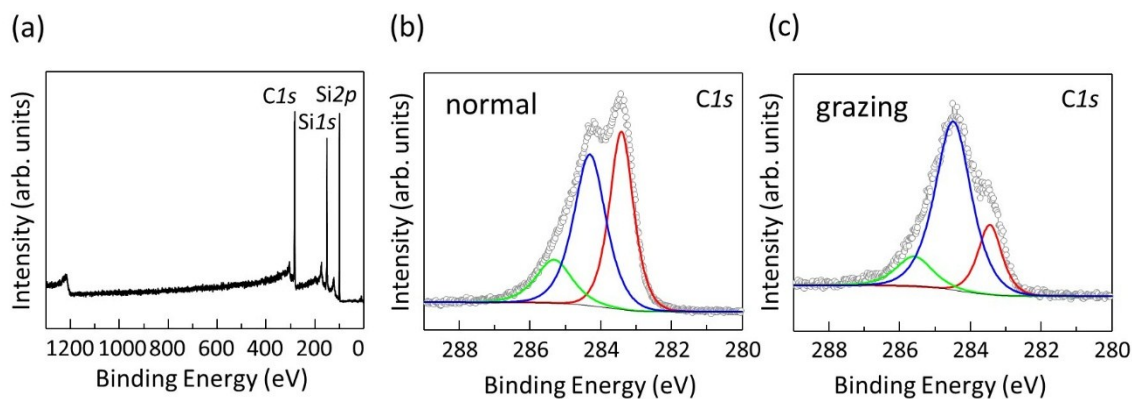


Figure S2. XPS spectra of the clean graphene/SiC(0001) surface. The survey scan (a) and the C 1s region (b) at normal incidence. C 1s region measured at grazing angle, 60° (c). Experimental data are shown by circles in panel b and c, while each component is represented by a continuous line. The spectra were calibrated by setting the SiC component of the C 1s region at 283.4 eV.⁵

3. X-ray Natural Linear Dichroism

3.1 XNLD measurements of TbPc₂ submonolayer on graphene/SiC(0001)

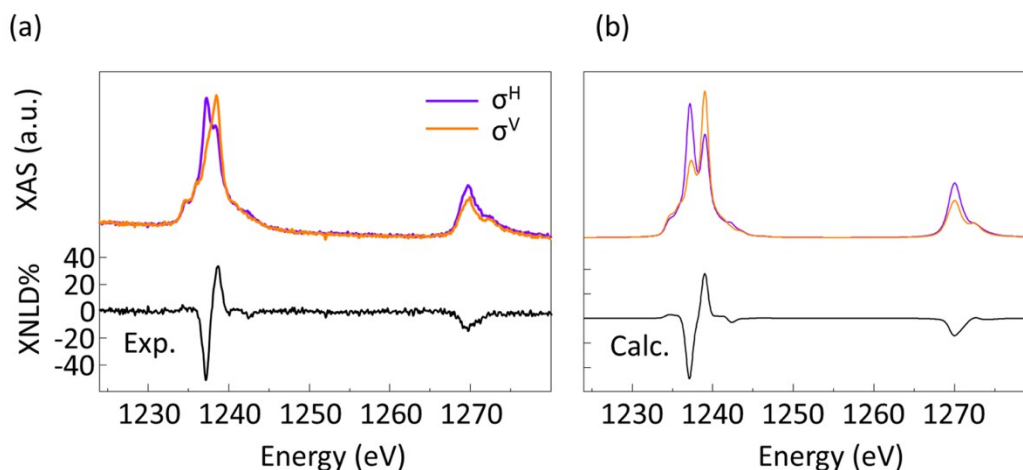


Figure S3. Experimental (a) and calculated (b) XNLD spectra recorded at $\theta = 45^\circ$ and $B = 3$ T. The strong dichroic XNLD signal at 1237 eV well matches the value reported for thin films of TbPc₂ at Au(111).⁷

Calculations assume a molecular distribution $\alpha = 15^\circ$ and an angle $\theta = 48^\circ$, matching the experimental angles within the experimental error. Measured data are in reasonable agreement with the calculations and in line with the XNLD intensity trend observed for $\theta = 0^\circ$ and 70° .

3.2 XNLD normalization

In order to normalize the XNLD spectra to the isotropic cross section of the dichroic system, the latter has been calculated starting from the experimental cross sections of the linear polarized light i.e. σ^V and σ^H for the vertical and horizontal polarization respectively.

We define $\mathbf{\epsilon}_V$ and $\mathbf{\epsilon}_H$ as the vertical and horizontal light polarization vectors, while σ^{\parallel} and σ^{\perp} are the cross sections measured with $\mathbf{\epsilon}$ parallel and perpendicular to \mathbf{n} , the surface normal, respectively.

Considering θ as the angle between the light propagation vector, \mathbf{k} , and \mathbf{n} , its complementary angle, θ' , is the angle formed by the $\mathbf{\epsilon}_H$ and \mathbf{n} (see Figure S4).

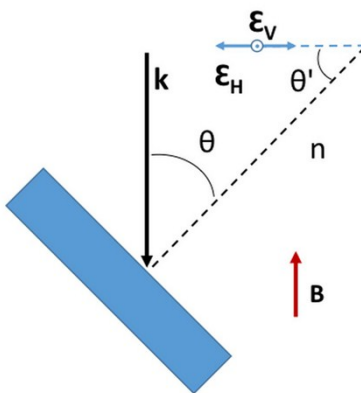


Figure S4. Scheme of the XNLD experiment.

The cross section can be generically defined⁸ as follows:

$$\sigma = (\cos \theta')^2 \sigma^{\parallel} + (\sin \theta')^2 \sigma^{\perp} \quad (S1)$$

Since the angle between $\mathbf{\epsilon}_V$ and \mathbf{n} is always 90°

$$\sigma^V = \sigma^{\perp}; \quad (S2)$$

while, for $\mathbf{\epsilon}_H$ forming a generic angle θ' with \mathbf{n} ,

$$\sigma^H = (\cos \theta')^2 \sigma^{\parallel} + (\sin \theta')^2 \sigma^{\perp} \quad (S3)$$

Starting from the definition⁸ of σ^{ISO}

$$\sigma^{ISO} = \frac{\sigma^{\parallel} + 2\sigma^{\perp}}{3} \quad (S4)$$

this can be rewritten as a function of the experimental cross section σ^H and σ^V as

$$\sigma^{ISO} = \frac{\sigma^H + [2(\cos \theta')^2 - (\sin \theta')^2]2\sigma^V}{3(\cos \theta')^2} \quad (S5)$$

In the case of $\theta=70^\circ$, σ^{ISO} is calculated considering $\theta'=20^\circ$, while for $\theta=45^\circ$ σ^{ISO} takes the form:

$$\sigma^{ISO} = \frac{2}{3}\sigma^H + \frac{1}{3}\sigma^V \quad (S6)$$

3.3 XNLD simulation

The normalized XNLD spectra were simulated starting from the scattering factors (σ^{\parallel} and σ^{\perp}) obtained by using crystal field multiplet theory (data from Margheriti et al.⁷) and reported in Figure S5.

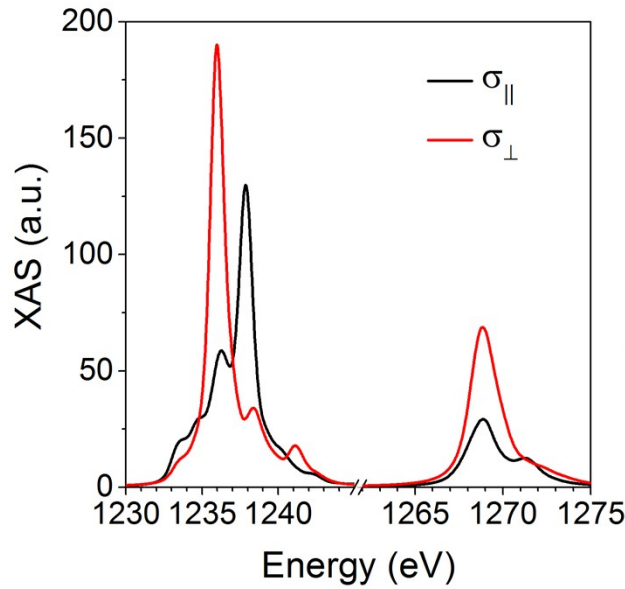


Figure S5. Simulated XAS spectra for linearly polarized light in the direction parallel (σ_{\parallel}) and perpendicular (σ_{\perp}) to the four-fold molecular axis. The spectra are calculated using crystal field multiplet theory (data from Margheriti et al.⁷).

To take into account the partial orientation of the molecules on the two substrate the distribution model developed by Perfetti et al.⁹ was employed here. The same model was used to simulate the magnetization of TbPc₂ monolayers, to be compared with the field dependence of XMCD intensity.

A distribution with in plane anisotropy was assumed, with the centre of the distribution defined by the angle α_0 formed by the fourfold molecular axis (easy axis of magnetization) and the normal to the surface (see Fig S6). We have assumed $\alpha_0 = 0^\circ$ for TbPc₂ on graphene/SiC and $\alpha_0 = 90^\circ$ for TbPc₂ on SiC in agreement with the sign of the XNLD signal and the anisotropy in the XMCD response.

The half width of the Gaussian distribution, σ in Fig. S6, was then adjusted to reproduce the intensity of the experimental signal by calculating the normalized XNLD signal by using eq. S2-S5 where the angle θ' is now not a unique value but it follows the distribution dictated by α_0 and σ .

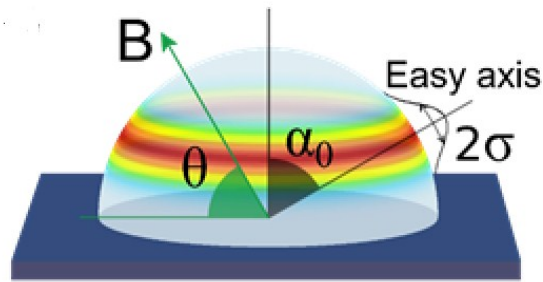


Fig S6. Model distribution of orientation of the TbPc₂ four-fold axis in a film characterized by an average angle α_0 with respect to the normal to the substrate and an isotropic in-plane orientation and a Gaussian distribution of half width σ .

4. X-ray Magnetic Circular Dichroism (XMCD)

4.1 XMCD measurements of TbPc₂ submonolayer on graphene/SiC(0001)

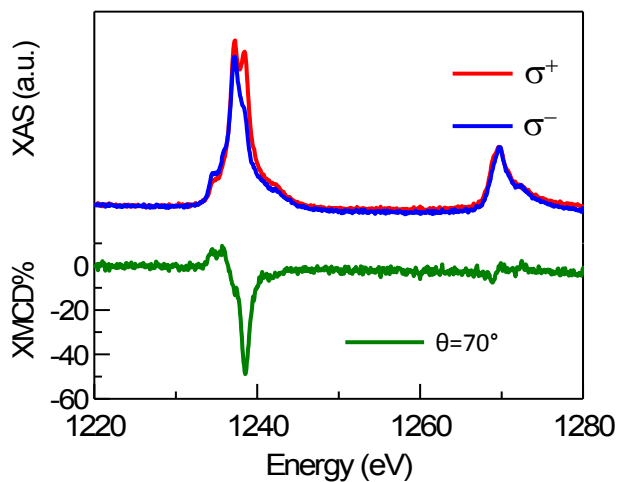


Figure S7. XAS (top panel) and XMCD (bottom) spectra recorded for TbPc₂ on graphene/SiC(0001) for the sample orientation $\theta = 70^\circ$ and at $B = 3$ T.

4.2 XMCD measurements of TbPc₂ submonolayer on SiC(0001)

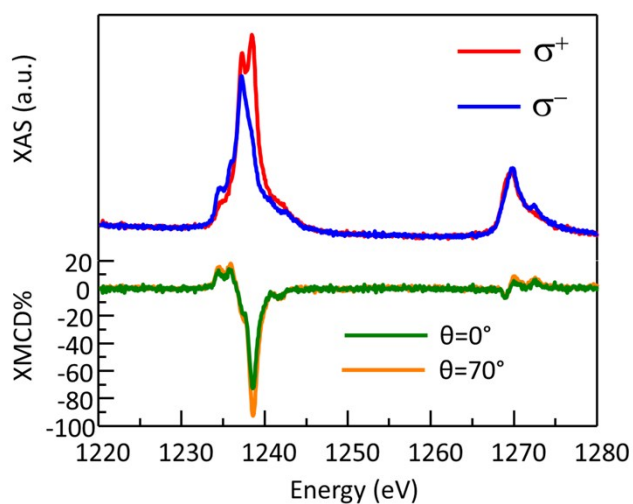


Figure S8. XAS (top panel) and XMCD (bottom) spectra recorded for TbPc₂ on SiC(0001). XMCD spectra are reported for the sample orientations $\theta = 0^\circ$ (green curve) and $\theta = 70^\circ$ (orange curve) at $B = 3$ T.

4.3 Simulation of the magnetization

The simulation of the equilibrium magnetization curves reported in Figure 3 of the main text was performed starting from the spin Hamiltonian

$$H = B_2^0 J_z^2 + B_4^0 J_z^4 + B_6^0 J_z^6 + gJ \cdot B$$

Where $B_2^0 = 414 \text{ cm}^{-1}$, $B_4^0 = -228 \text{ cm}^{-1}$, $B_6^0 = 33 \text{ cm}^{-1}$ as in *Ishikawa et al.*¹⁰ The inclusion of transverse terms has no effect in the static properties at the investigated temperatures.

To take into account the partial orientation of the molecules on the different substrates a weighted average of the contributions coming from the distribution depicted in Fig. S6 was assumed, with the α_0 and σ parameters extracted from the simulation of the XNLD spectra.

References

- 1 E. Pallecchi, F. Lafont, V. Cavaliere, F. Schopfer, D. Mailly, W. Poirier and A. Ouerghi, *Sci. Rep.*, 2014, **4**, 4558.
- 2 D. E. Andrifi, M. E. Cian, H. D. I. Moussavi and A. N. Fischer, *Inorg. Chem*, 1985, **24**, 3162–3167.
- 3 K. Katoh, Y. Yoshida, M. Yamashita, H. Miyasaka, B. K. Breedlove, T. Kajiwara, S. Takaishi, N. Ishikawa, H. Isshiki, Y. F. Zhang, T. Komeda, M. Yamagishi and J. Takeya, *J. Am. Chem. Soc.*, 2009, **131**, 9967–9976.
- 4 C. Riedl, U. Starke, J. Bernhardt, M. Franke and K. Heinz, *Phys. Rev. B*, 2007, **76**, 245406.
- 5 B. Lalmi, J. C. Girard, E. Pallecchi, M. Silly, C. David, S. Latil, F. Sirotti and A. Ouerghi, *Sci. Rep.*, 2014, **4**, 4066.
- 6 A. Ouerghi, M. G. Silly, M. Marangolo, C. Mathieu, M. Eddrief, M. Picher, F. Sirotti, S. El Moussaoui and R. Belkhou, *ACS Nano*, 2012, **6**, 6075–6082.
- 7 L. Margheriti, D. Chiappe, M. Mannini, P.-E. Car, P. Saintavit, M.-A. Arrio, F. B. de Mongeot, J. C. Cezar, F. M. Piras, A. Magnani, E. Otero, A. Caneschi and R. Sessoli, *Adv. Mater.*, 2010, **22**, 5488–5493.
- 8 C. Brouder, *J. Phys. Condens. Matter*, 1990, **2**, 701–738.
- 9 M. Perfetti, M. Serri, L. Poggini, M. Mannini, D. Rovai, P. Saintavit, S. Heutz and R. Sessoli, *Adv. Mater.*, 2016, **28**, 6946–6951.
- 10 Naoto Ishikawa, Miki Sugita, Tomoko Okubo, Naohiro Tanaka, A. Tomochika Iino and Y. Kaizu*,

Inorg. Chem., 2003, **42**, 2440–2446.